First-principles calculation of the electronic structure of the wurtzite semiconductors ZnO and ZnS

Peter Schröer, Peter Krüger, and Johannes Pollmann
Institut für Theoretische Physik II, Universität Münster, D-4400 Münster, Germany
(Received 28 September 1992)

We report *ab initio* calculations of the lattice constants and the electronic band structure of the hexagonal wurtzite-structure semiconductors ZnO and ZnS. We employ the local-density approximation and solve the Kohn-Sham equations for nonlocal, separable, and norm-conserving pseudopotentials self-consistently. We use basis sets of localized Gaussian orbitals with s, p, d, and s^* symmetry. In particular, we investigate the influence of the Zn $3d$ electrons on the results for the lattice constants and the band structure. Results of calculations employing both Zn^{2+} and Zn^{12+} ionic pseudopotentials are presented and discussed. For ZnS, both the cubic zinc blende and the hexagonal wurtzite polytype have been studied. The calculated lattice constants are found to be in excellent agreement with experiment for both semiconductors when the d electrons are explicitly taken into account as valence electrons. The agreement of the calculated bands of ZnS with experimental data and with the results of a plane-wave calculation from the literature using about 6.000 plane waves for the cubic crystal is very good except for the absolute energy position of the d bands. For ZnO the calculated bands agree better with angle-resolved photoemission data when the Zn^{12+} pseudopotential is employed. The agreement, however, is still far from satisfactory and the calculated absolute position of the d bands is off, again. The discrepancies seem to be related to correlation effects in the narrow d bands. We find the Zn $3d$ electrons to strongly interact with the O $2p$ electrons in ZnO. According to our results, the p-d mixing in ZnO is about twice as large as in ZnS.

I. INTRODUCTION

ZnO is a compound semiconductor whose ionicity resides exactly at the borderline between covalent and ionic semiconductors. It is at the "ionic extreme" of tetrahedrally coordinated compound semiconductors whose zinc-blende or wurtzite structures lead to their classification as covalently bonded bulk materials. ZnO is thus the prototype of tetrahedrally coordinated, ionic II-VI compound semiconductors. Other materials of this group, are e.g., ZnS, CdS, or CdSe. The prototypic ZnO has been the subject of detailed experimental and theoretical investigations.[1-8] Nevertheless, a first-principles calculation of the electronic and structural properties using modern *ab initio* pseudopotentials is missing for this wurtzite semiconductor as well as for hexagonal ZnS. This is probably related to the fact that the four basis atoms in the hexagonal unit cell require an enormous number of plane-wave basis states for a convergent description since strongly localized wave functions and pseudopotentials are involved. ZnO is one of the worst cases for a pseudopotential description since both the O $2p$ and Zn $3d$ orbitals are the lowest-lying orbitals of the respective symmetry type. Therefore the screening of the nuclear charge by core electrons is very incomplete in both cases. The oxygen pseudopotential cannot be orthogonalized on lower-lying p states and the zinc pseudopotential cannot be orthogonalized on lower-lying d states. Both pseudopotentials and the related wave functions are strongly localized. Oxygen has very tightly bound $2p$ electrons and Zn has very tightly bound $3d$ electrons which sense the nuclear attraction very efficiently. A proper description of the O $2p$ and the Zn $3d$ valence electrons thus enforces a considerable numerical effort.

In many earlier attempts to calculate the ZnO band structure, the Zn $3d$ electrons have been considered as core electrons, reducing the numerical effort drastically when a plane-wave basis set is used. This reduction in computer time and program size has had its price. Former calculations[9-12] could not estimate the contribution of the Zn $3d$ electrons to the bonding properties in the wurtzite semiconductors ZnO and ZnS. Further shortcomings of these approaches will be commented on further below. The lack of a reliable bulk description led to controversies about the nature and origin of possible surface states at the ZnO $(10\bar{1}0)$ surface.[6,7] An *ab initio* study of the above-mentioned crystals can thus provide useful information on the nature of their electronic bulk states and it is a mandatory prerequisite for state of the art surface band-structure calculations of wurtzite-structure ZnO and ZnS. In addition, total energy calculations yield theoretical lattice constants. They indicate how well ground-state properties of ZnO and ZnS are described within the local-density approximation (LDA).

The paper is organized as follows. In Sec. II we briefly summarize the ingredients of the calculations and in Sec. III we present our results for ZnS and ZnO. There is only very rare experimental information on the less popular hexagonal wurtzite phase of ZnS. We calculate, therefore, the band structure for the cubic modification of ZnS as well, and compare our results with experimental data obtained for this modification.[13,14] The atoms are tetrahedrally coordinated in both polytypes so that the nearest-neighbor configurations are the same. The calculated electronic band structure of ZnO is compared with the results of angle-resolved photoemission spectroscopy

(ARPES) data.[2] A short summary in Sec. IV concludes the paper and details on the calculation of matrix elements using separable pseudopotentials are given in the Appendix.

II. METHOD OF CALCULATION

Our calculations are performed in the framework of local-density theory within the local-density approximation.[15] We have used nonlocal, norm-conserving pseudopotentials[16] in the separable form as suggested by Kleinman and Bylander.[17] In order to study the influence of the Zn $3d$ electrons on the lattice constants and the band structure, we have carried out two different calculations. First, we consider the Zn $3d$ electrons as core electrons, i.e., we use a Zn^{2+} ionic pseudopotential. Second, we incorporate the Zn $3d$ electrons as valence electrons using a Zn^{12+} ionic pseudopotential. The Zn^{2+},O^{6+}, and S^{6+} pseudopotentials are taken from the tables published by Stumpf, Gonze, and Scheffler.[18] In addition, we have generated a Zn^{12+} pseudopotential (not tabulated in Ref. 18) following the prescriptions of Gonze, Käckell, and Scheffler[19] with the s part of the potential chosen as the local component to avoid ghost states. We use the Ceperley-Alder[20] form of the exchange and correlation energy as parametrized by Perdew and Zunger.[21]

The wave functions are expanded in terms of linear combinations of Gaussian orbitals (LCGO) consisting of Bloch sums of atom-centered Gaussians times a polynomial having s, p, d, or s^* symmetry. The s^* orbital denotes the polynomial r^2 representing the s-like "trace" of d states.[22] For ZnS it turned out to be sufficient to use two s, p, d, and s^* shells with decay constants of 0.2 and 0.6 (all length being measured in atomic units) to represent the orbitals at each Zn atom when the Zn^{2+} pseudopotential is used. For the S orbitals we use three s, p, and s^* shells with decay constants of 0.2, 0.5, and 0.8. With two Zn and two S atoms in the unit cell, this amounts to 70 basis states so that 70×70 matrices have to be diagonalized for each wave vector $\mathbf{k}$. When the Zn^{12+} pseudopotential is employed, a larger basis set is necessary to represent the extremely localized Zn $3d$ valence electrons. In this case the Zn orbitals are represented by two s, p d, and s^* shells with decay constants of 0.17 and 0.5 and three additional d shells with decay constants of 2, 6.6, and 20 to properly describe the highly localized occupied $3d$ states. This yields 35 basis functions for each Zn atom while the number of S basis states remains unchanged. Thus our band-structure calculations with Zn^{12+} ionic pseudopotentials for hexagonal ZnS require the diagonalization of 100×100 matrices. In cubic ZnS 50×50 matrices occur since there is only one Zn and one S atom in the unit cell. In the calculations for ZnO we use the respective number of Zn basis states for the two different ionic pseudopotentials. The O orbitals are described in this case by three s, p, and s^* shells with decay constants of 0.3, 0.9, and 3.5. Thus, also for ZnO our calculations require diagonalizations of 70×70 (Zn^{2+} pseudopotential) or 100×100 (Zn^{12+} pseudopotential) matrices, respectively. To test an improved description of the localized nature of the O $2p$ orbitals, we have in addition carried out calculations using five s, p, d, and s^* shells per O atom yielding 170×170 Hamiltonian matrices. The deviations of the resulting bands from those calculated with the three s, p, and s^* shell oxygen basis turned out to be less than 0.15 eV. The results presented in this paper have been calculated, therefore, with the smaller basis set for the O atoms.

The local part of the pseudopotentials is of long range. Therefore it is convenient to carry out the computation of the Hamiltonian matrix elements for this part of the potential in momentum space. The matrix elements of the short-range nonlocal part of the pseudopotential, on the contrary, can efficiently be evaluated in real space due to their separable form. Details are given in the Appendix. The total energy of the system is determined using the momentum-space formalism of Ihm, Zunger, and Cohen.[23] This method involves integrations over the Brillouin zone which are carried out using six (ten) special $\mathbf{k}$ points[24] within the irreducible wedge of the Brillouin zone for the wurtzite (zinc-blende) structure. The charge density is calculated in real space on a grid with spacings of nearly 0.1 Å corresponding to $31\times31\times51=49\,011$ points in the real-space unit cell when the localized Zn $3d$ electrons are included. A subsequent transformation into momentum representation is efficiently carried out using the fast-Fourier-transform algorithm.[25]

To test the appropriateness and the flexibility of our LCGO basis sets, we have performed plane-wave band-structure calculations for hexagonal ZnS using the Zn^{2+} ionic pseudopotential, in addition. Convergent results are obtained with 840 plane waves corresponding to an energy cutoff of 21 Ry. The band structure calculated with only 70 localized Gaussian orbitals agrees to within 0.1 eV with the plane-wave results.

III. RESULTS AND DISCUSSION

Before we start to discuss specific results for the solids, it is worthwhile to take a look at the energy levels of the isolated O, S, and Zn atoms forming ZnO and ZnS. The LDA energy levels of the various states are summarized in Table I. The oxygen $2s$ states and the sulfur $3s$ states reside very low in energy as compared to the other states of the three atoms. They can be expected to yield narrow bands way below the valence bands of the semiconductors and to show very little hybridization with the other states. The remaining states give rise to the valence and lower conduction bands of ZnO and ZnS. We note that the Zn $3d$ electrons reside 3.3 eV in energy below the S $3p$ electrons but only 1.2 eV below the O $2p$ electrons. The energy gaps for both ZnS and ZnO predominantly result

TABLE I. Atomic LDA energy levels for various states of O, S, and Zn, in eV.

O		S		Zn	
E_{2p}	−9.2	E_{3p}	−7.1	E_{4p}	−1.5
E_{2s}	−23.8	E_{3s}	−17.3	E_{4s}	−6.2
				E_{3d}	−10.4

from a bonding-antibonding interaction between the anion p states and the cation $4s$ states. The mainly p-like bonding states at the anions are pushed down and the mainly s-like antibonding states at the cation are pushed up in energy by this interaction. In consequence, the anion p states are shifted even closer to the Zn $3d$ energy level and we can expect that the O $2p$ states become nearly resonant with the Zn $3d$ states because of their small initial energy separation of only 1.2 eV (see Table I). Therefore a considerably stronger p-d hybridization will occur in ZnO, as compared to ZnS, and correlation effects which are typical for narrow d bands might turn out to be much more important in ZnO than in ZnS.

A. ZnS

Let us begin our discussion with the hexagonal wurtzite-structure crystal ZnS. In this case we expect less-pronounced influences of the Zn $3d$ electrons in the anion-derived valence bands due to the simple energetic considerations mentioned above. We first address the results for the case where the $3d$ electrons are treated as core electrons.

1. Calculations using a Zn^{2+} pseudopotential

For the lattice constants of hexagonal ZnS we obtain in this case $a=3.34$ Å and $c=5.43$ Å. The respective experimental lattice constants[13] are 3.82 and 6.26 Å. Our calculated values are about 13% too small as compared to the experimental data. At the first glance, this discrepancy is rather astonishing, since LDA calculations within the *ab initio* pseudopotential scheme yield lattice constants in excellent agreement with experiment[26] for a wide class of materials. The above discrepancy should therefore not be attributed to the LDA but rather to the use of an ionic Zn^{2+} pseudopotential. In fact, the treatment of the Zn $3d$ electrons as core electrons in a Zn^{2+} pseudopotential is based on the assumption that the closed $3d$ shell is chemically inert. This, however, is not justified, as we will show below. The same has been noted for other IIB-VI compounds[27,28] and for a III-V compound[29] whose outermost cation d bands occur within the valence-band spectra. Also for those systems the calculated equilibrium lattice constants turned out to be incorrect if the repulsion of the cation d electrons was neglected. Moreover, such calculations fail to predict the essential electronic features correctly. Wei and Zunger have discussed this phenomenon for zinc-blende structure IIB-VI compound semiconductors.[28] The same obtains for wurtzite-structure ZnS and ZnO as we will show in this paper.

Let us now move on to the electronic structure. In Table II we show electronic eigenvalues of wurtzite ZnS at the Γ point and of zinc blende ZnS at the Γ and L points calculated with the Zn^{2+} pseudopotential. For the zinc-blende structure experimental data are available and they are shown for comparison in Table II as well. First we note that respective energy levels for both structures are similar. At the same time we realize that the measured binding energy of the Γ_{1v} and L_{1v} states is about 2 eV larger than that calculated with the Zn^{2+} pseudopotential. Further shortcomings of these calculations become obvious when the respective theoretical and experimental data for zinc-blende ZnS are compared. The width of the mainly anion-p-derived valence bands (L_{1v}), e.g., is significantly underestimated by 1.2 eV and many further discrepancies can be seen in Table II. Amazingly enough, the calculated energy gap of 3.55 eV compares favorably with the measured value of 3.8 eV for cubic ZnS, in marked contrast to the general experience that LDA calculations usually yield gap energies which are only 50% or less of the experimental gap. In view of all the other discrepancies mentioned above, this near agreement for the gap energy calculated with the Zn^{2+} pseudopotential has to be viewed as purely fortuitous. Of course, we cannot directly compare our results for hexagonal ZnS with the experimental data for cubic ZnS. It is nevertheless useful to compare the theoretical results for both structures with one another. As mentioned already, the energy positions of the sulfur s states and the widths

TABLE II. Electronic eigenvalues (in eV) of wurtzite and zinc-blende ZnS for Zn^{2+} and Zn^{12+} pseudopotential calculations in comparison with the plane wave (PW) results of Ref. 32 and experimental data from Ref. 13. The experimental position of the d bands is taken from Ref. 14. The center of gravity of the d bands in wurtzite is noted with E (Zn $3d$). The experimental lattice constants are used in these calculations.

	Wurtzite			Zinc blende			
	Zn^{2+}	Zn^{12+}		Zn^{2+}	Zn^{12+}	Zn^{12+}	
ZnS	LCGO	LCGO	ZnS	LCGO	LCGO	PW	Expt.
Γ_{1v}	−12.09	−13.22	Γ_{1v}	−11.60	−13.14	−13.07	−13.5
Γ_{3v}	−11.11	−12.24	L_{1v}	−10.65	−12.19	−12.10	−12.4
Γ_{3v}	−4.45	−5.30	L_{1v}	−4.31	−5.14	−5.43	−5.5
Γ_{6v}	−0.67	−0.91	L_{3v}	−0.61	−0.89	−0.90	−1.4
Γ_{5v}	0.00	0.00	Γ_{15v}	0.00	0.00	0.00	0.0
Γ_{1c}	3.23	1.97	Γ_{1c}	3.55	1.77	1.84	3.9^{W}, 3.8^{ZB}
Γ_{3c}	3.89	3.44	L_{1c}	4.43	3.03	3.05	
Γ_{5c}	6.94	7.21	Γ_{15c}	7.06	6.20	6.15	8.3
E(Zn$3d$)		−5.8	Γ_{15d}		−5.84	−6.63	∼−9.0
			Γ_{12d}		−5.27	−6.16	∼−9.0

of the mainly anion-derived valence bands turn out to be similar in both cases. This is understandable in terms of the fact that the tetrahedral nearest-neighbor configurations are the same in both cases. Furthermore we observe that the calculated gap of 3.55 eV for the zinc-blende modification is larger than the respective value of 3.23 eV for the hexagonal crystal. This trend is in marked disagreement with experiment which yields gap energies of 3.8 eV for cubic and 3.9 eV for hexagonal ZnS.

Summarizing the results presented so far, we have to conclude that a description of ZnS using a Zn^{2+} pseudopotential fails to predict the basic features of the electronic structure as well as the equilibrium lattice constants. In order to improve the results it is obviously necessary to treat the Zn $3d$ electrons as what they are, namely as valence electrons.

2. *Calculations using a Zn^{12+} pseudopotential*

Employing our separable Zn^{12+} ionic pseudopotential for ZnS, we obtain for the two lattice constants $a=3.79$ Å and $c=6.19$ Å in excellent agreement with experiment. The deviations are roughly 1%. A slight underestimate of the lattice constants is typical for LDA calculations when the Ceperley-Alder form of the exchange-correlation energy is used. We thus find that orthogonalization effects, p-d interactions, and cationic d-d repulsions increase the lattice constants by roughly 13%.

The electronic eigenvalues for both polytypes of ZnS resulting for the Zn^{12+} potential are given in Table II as well. First we note that now the calculated energy levels of the sulfur s bands (Γ_{1v},L_{1v}) agree very well with experiment. The general finding that respective energy levels are very similar for cubic and hexagonal ZnS is confirmed, in addition, illustrating the similarity of both polytypes. The calculated gap energies now show the typical LDA behavior amounting to roughly 50% of the measured gaps. It is noteworthy, in particular, that now the gap for the wurtzite-structure crystal turns out to be larger (1.97 eV) than that of the zinc-blende-structure crystal (1.77 eV), in agreement with the experimentally observed trend. Comparing the results for the cubic ZnS with experiment, we see that the overall agreement between theory and experiment is good. The position of the sulfur s band (Γ_{1v}) is close to experiment and the width of the upper valence bands (L_{1v}) is increased by nearly 0.7 eV as compared with the results from the Zn^{2+} pseudopotential calculations. The dispersion of the highest valence band (L_{3v}) now is larger, but it is still somewhat underestimated. The unoccupied conduction-band states (see, e.g., Γ_{15c}) are in good agreement with experiment—given a general 2-eV offset error in the LDA theory for the conduction states of ZnS. For a discussion of the "gap problem" in LDA, see, e.g., Refs. 30 and 31. The energy values of the Zn $3d$ bands are given in Table II as well. They are more than 3 eV higher in energy as compared to experiment. We will comment on this point in more detail further below.

Let us digress for a moment from the discussion of physical features and address a more formal point of the calculations. One of the big advantages of using LCGO basis sets is the fact that inclusion of localized d orbitals does not increase the number of basis states drastically. As we mentioned already in the Introduction, the use of a Zn^{12+} potential increases our basis set only from 70 to 100 Gaussian orbitals for hexagonal ZnS. This is in marked contrast to the case of plane-wave calculations. For the Zn^{2+} potential in hexagonal ZnS we obtain essentially the same results with 70 Gaussian orbitals as with 840 plane waves in the set, as mentioned already. With the Zn^{12+} potential employed for cubic ZnS, Martins, Troullier, and Wei[32] have shown that a set of about 6.000 plane waves (corresponding to an energy cutoff of 121 Ry) is necessary for convergence. The need of such a huge basis set for the bulk electronic structure already renders surface calculations basically unfeasible with plane waves. We remind the reader that we need only 50 localized Gaussian orbitals in our LCGO basis set for cubic ZnS. The eigenvalues obtained by Martins, Troullier, and Wei for cubic ZnS are shown in Table II for comparison. It is amazing to see how extremely well our results agree with those of Ref. 32. The only noteworthy difference occurs in the position of the d bands, which is 0.8–0.9 eV lower in the plane-wave results as compared to our results. This can be due to the use of slightly different pseudopotentials.

The band structure for hexagonal ZnS resulting from our calculations with the Zn^{12+} pseudopotential is shown in Fig. 1 together with the density of states (DOS) as calculated using the Raubenheimer-Gilat scheme.[33] We have used 1156 **k** points for sampling. Around -12.5 eV, we obtain the two sulfur s bands which show weak dispersions. Next, we observe at the top of the heteropolar gap the ten, mostly Zn $3d$-derived, valence bands which are centered around -5.8 eV. They are split into two groups of bands leading to a double-peak structure in the DOS. The d bands are very narrow and show only very weak dispersion. Their width is roughly 1 eV. This bandwidth results from the p-d hybridization with the S

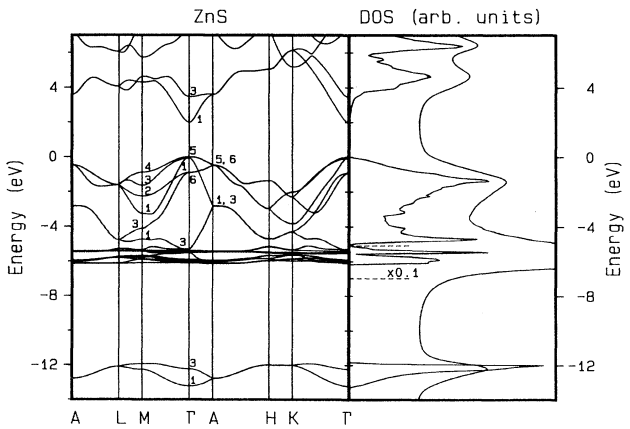

FIG. 1. Band structure and density of states for hexagonal ZnS calculated with a Zn^{12+} pseudopotential. Additionally a Lorentzian-broadened DOS ($\gamma=0.3$ eV) is plotted. The unbroadened DOS resulting for the d bands is scaled down by a constant factor of 0.1.

$3p$ bands and from the obviously weak second-nearest-neighbor cation-cation d-d interaction. The calculated d bands result 3.2 eV higher in energy than observed experimentally.[14] This is certainly due to shortcomings in LDA when highly localized states are to be described. Similar discrepancies have been found in local spin density (LSD) calculations for $3d$ transition metal oxides (see, e.g., Ref. 34). Furthermore, part of the discrepancy could be related to the fact that in photoemission measurements of highly correlated electrons from narrow d bands electronic relaxation effects (hole relaxation[30]) occur which give rise to relaxation shifts. They are neglected in a one-particle band model. The following six valence bands are mainly S $3p$-derived states and the lower conduction band has strong Zn $4s$ contributions. In order to estimate the importance of p-d hybridization we have analyzed the various contributions to the wave functions of the six uppermost valence bands. Characteristic results for a few **k** points are shown in Table III. We see that there is about 15% d admixture in many of the S $3p$-derived valence bands except for some cases, where the d admixture is much larger (M_{1v} and Γ_{3v}) due to resonant p-d coupling. The amount of only 15% p-d hybridization explains the relatively narrow width of the d bands of only 1 eV. For cubic II-VI compound semiconductors the effects of p-d coupling have been analyzed in detail by Wei and Zunger.[28]

In spite of the difference between the measured and calculated d-band positions, originating from correlation effects ignored in LDA, the explicit consideration of the Zn $3d$ electrons as valence electrons dramatically improves the quality of our results. The lattice constants agree extremely well with the measured data, the energies of the sulfur s states are correct, and a number of calculated eigenvalues agree nicely with experiment. Furthermore, the hybridization interaction of the d electrons with anion p electrons leads to a repulsion of the involved states. In consequence an increased width of the upper valence bands and a decrease of the optical gap results. The latter occurs because the S $3p$ states are pushed up in energy towards the Zn $4s$-derived conduction bands by the p-d interaction. Finally, there is an important formal aspect to be noted. If a Zn^{2+} pseudopotential is employed, treating the Zn $3d$ electrons as core electrons, this implies a linearization of the explicitly nonlinear exchange and correlation energy. In consequence, errors in the calculated eigenvalues due to significant overlap between the $3d$ electrons and the p valence electrons occur. These errors are automatically avoided when the Zn^{12+} potential is used. In summary we conclude that the explicit inclusion of the Zn $3d$–S $3p$ interactions by the use of a Zn^{12+} pseudopotential is essential for a correct description of ZnS. This finding is confirmed by additional calculations which we have carried out in order to test a partial core-correction scheme[35] which avoids linearization of the exchange and correlation energy but neglects the p-d hybridization. Our results are in accordance with the findings of Engel and Needs[36] who have shown for cubic ZnS that the inclusion of partial core-corrections leads to an increase of the lattice constant from 4.72 (Zn^{2+}) to 5.19 Å. This value is still 4% smaller than the experimental value of 5.404 Å.[13] Using Zn^{12+} pseudopotentials Martins and Troullier obtain a lattice constant of 5.35 Å and we find a lattice constant of 5.36 Å.

TABLE III. Wave-function analysis for the upper six valence bands of wurtzite ZnS at representative **k** points. The percental orbital contributions are given.

ZnS	S($3p$)	S($3s$)	Zn($3d$)	Zn($4s$)	Zn($4p$)
$A_{1,3v}$	41.3	4.7	22.6	22.9	8.3
$A_{5,6v}$	77.6	0.0	13.9	0.0	8.5
M_{1v}	26.9	2.9	46.7	21.0	2.5
M_{3v}	39.2	2.4	22.0	29.8	6.6
M_{1v}	61.3	0.4	11.3	5.9	21.0
M_{2v}	72.2	0.0	6.6	0.0	21.2
M_{3v}	63.8	0.1	17.4	0.2	18.5
M_{4v}	76.2	0.0	11.7	0.0	12.0
Γ_{3v}	7.5	1.0	80.9	9.8	0.7
Γ_{6v}	75.2	0.0	12.4	0.0	12.5
Γ_{1v}	82.8	0.0	13.5	0.2	3.5
Γ_{5v}	80.8	0.0	16.5	0.0	2.7

B. ZnO

In ZnO the energetic separation between the p- and d-valence electrons is very small, so that pronounced effects of the d states can be expected. Indeed, also in this case we observe distinct differences between the results of the calculations using Zn^{2+} or Zn^{12+} ionic pseudopotentials, respectively, which we will discuss now in direct comparison without introducing the respective subsections as in Sec. III A. The theoretical lattice constants as resulting for the two potentials are given in Table IV together with the results for ZnS discussed already in Sec. III A. The calculated lattice constants of ZnO resulting with the Zn^{2+} pseudopotential are as much as 18% too small as compared to the experimental values. This underestimate is even larger than for ZnS. Using the Zn^{12+} potential we obtain theoretical lattice constants which nearly coincide with the experimental values. Explicit inclusion of the $3d$ states thus widens the ZnO lattice even more than the ZnS lattice. This is a first hint to an increased importance of the d states. The smaller lattice constants of ZnO as compared to ZnS (see Table IV) are due to the fact that the O $2p$ orbitals are more tightly bound and thus stronger localized than the S $3p$ orbitals.

TABLE IV. Lattice constants of wurtzite ZnS and ZnO (in Å). The theoretical values are calculated with the use of Zn^{2+} and Zn^{12+} pseudopotentials, respectively. The experimental data are taken from Ref. 13.

		Zn^{2+}	Zn^{12+}	Expt.
ZnS	a	3.34	3.79	3.82
	c	5.43	6.19	6.26
ZnO	a	2.65	3.23	3.25
	c	4.24	5.18	5.21

The electronic band structure calculated with the Zn^{12+} pseudopotential is shown in Fig. 2 together with the DOS. Around -18 eV we obtain two s bands originating from the s states at the two O atoms in the unit cell. Next we observe from -6.5 to -4 eV ten bands with strong d character originating mostly from the Zn $3d$ states. The next group of six valence bands mainly stems from the O $2p$ states and the lowest conduction bands have strong Zn $4s$ contributions. We see in Fig. 2 that the top of the d bands now occurs just 4 eV below the top of the valence bands limiting the width of the Zn $4s$- and O $2p$-derived upper six valence bands to 4 eV. It is perfectly reasonable that the d bands in the ZnO result closer to the anion-p-derived valence bands than in ZnS since the energy difference between the respective p and d levels (see Table I) is only 1.2 eV in ZnO as compared to 3.3 eV in ZnS. The d bands show a remarkable dispersion and separate again into two groups of bands with a total width of 2.5 eV. This strong increase in the d-band width, as compared to ZnS, is due to a significantly stronger p-d interaction in ZnO. ARPES data of Zwicker and Jacobi[2] show a double-peak structure in the energy range between -9.5 and -6.0 eV originating from the Zn $3d$ bands. The two groups of six and four d bands are thus resolved in experiment. Also the calculated width of 2.5 eV agrees well with the data since the inherent broadening of the spectra has to be taken into account (see the broadened DOS in Fig. 2 for that matter). The full width at half maximum in both the spectra[2] and the broadened DOS is 2.5 eV. The absolute position of the calculated d bands is considerably higher than observed in experiment, again. The explanation for this discrepancy in terms of correlation effects in the d bands, given in Sec. III A for ZnS, obtains equally well for ZnO. But in the latter case the d bands reside energetically about 1.5 eV closer to the anion-derived p bands. The inaccuracies in the description of the d bands, therefore, have a much stronger influence on the anion-derived p valence bands in ZnO than in ZnS. This conjecture is borne out by the eigenvalues given in Table V and, in particular, by the results of a wave-function analysis given in Table VI for a few high-symmetry points. In Table V results of calculations with both the Zn^{2+} and the Zn^{12+} pseudopotentials are given. Similar differences in the results of these two calculations can be observed, in general, as discussed for ZnS in connection with Table II. Using the Zn^{2+} potential, we find a value of 2.13 eV for the fundamental gap which is about 30% smaller than the experimental value of 3.4 eV.[13] Again this "degree of agreement" is purely accidental. When the d bands are explicitly included in the valence bands (see the Zn^{12+} results in Table V) we find the same type of changes as discussed already for ZnS. There is, however, a noteworthy feature to be observed. While the calculated gap energy for the Zn^{12+} potential was roughly 50% of the experimental value in ZnS, it is now only about 7% of the experimental value. We find a gap energy of only 0.23 eV (see Fig. 2 and Table V), i.e., to say that the gap has almost closed. This is due to the very strong p-d interactions which push the O $2p$-derived valence states very close to the Zn $4s$-derived conduction states. Exactly the same behavior has been found in LSD results for $3d$ transition metal oxides (see, e.g., Ref. 34). In that case, the local spin density cal-

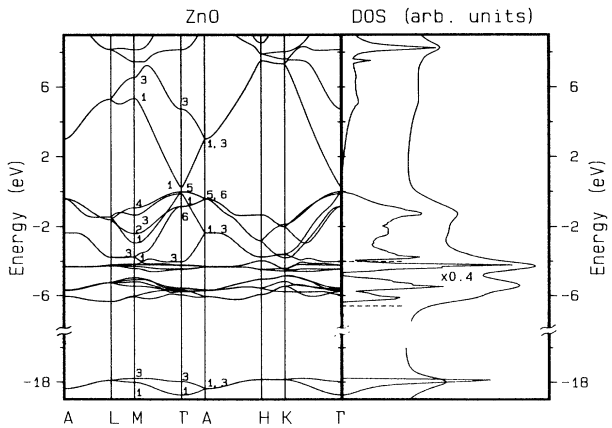

FIG. 2. Band structure and density of states for ZnO calculated with a Zn^{12+} pseudopotential. Additionally a Lorentzian-broadened DOS ($\gamma=0.3$ eV) is plotted. The unbroadened DOS resulting for the d bands is scaled down by a constant factor of 0.4.

TABLE V. Electronic eigenvalues of ZnO obtained from Zn^{2+} and Zn^{12+} pseudopotential calculations (in eV). The last column differs from the preceding one by the use of a X_α potential ($\alpha=0.9$) instead of the Ceperley-Alder exchange-correlation potential. All calculations are performed for the experimental lattice constants.

	ZnO	Zn^{2+}	Zn^{12+}	X^α
Γ	Γ_{1v}	−17.08	−18.75	−18.09
	Γ_{3v}	−16.24	−17.97	−17.42
	E (Zn3d)		−5.17	−5.90
	Γ_{3v}	−4.32	−4.03	−4.65
	Γ_{6v}	−0.65	−0.85	−0.73
	Γ_{1v}	0.0	−0.12	−0.05
	Γ_{5v}	−0.11	0.0	0.0
	Γ_{1c}	2.13	0.23	1.58
	Γ_{3c}	6.64	4.71	6.04
M	M_{1v}	−16.31	−18.02	−17.46
	M_{3v}	−16.05	−17.78	−17.26
	E(Zn 3d)		−4.99	−5.74
	M_{1v}	−3.96	−3.76	−4.12
	M_{3v}	−3.03	−3.75	−3.44
	M_{1v}	−2.35	−2.95	−2.67
	M_{2v}	−1.63	−2.42	−2.03
	M_{3v}	−1.08	−1.35	−1.18
	M_{4v}	−0.58	−0.93	−0.77
	M_{1c}	7.16	5.34	6.49
	M_{3c}	8.50	6.55	7.90
A	$A_{1,3v}$	−16.70	−18.37	−17.76
	E(Zn 3d)		−5.21	−5.98
	$A_{1,3v}$	−2.62	−2.37	−2.35
	$A_{5,6v}$	−0.38	−0.43	−0.36
	$A_{1,3c}$	4.88	3.02	4.14

TABLE VI. Wave-function analysis for the upper six valence bands of wurtzite ZnO at representative **k** points. The percental orbital contributions are given.

ZnO	O(2p)	O(2s)	Zn(3d)	Zn(4s)	Zn(4p)
$A_{1,3v}$	28.4	3.4	45.7	18.4	4.1
$A_{5,6v}$	68.4	0.0	27.7	0.0	3.6
M_{1v}	10.9	2.0	80.6	5.1	1.3
M_{3v}	35.0	0.9	44.5	14.1	5.5
M_{1v}	41.0	0.1	41.3	5.5	12.0
M_{2v}	57.7	0.0	27.4	0.0	14.9
M_{3v}	54.3	0.2	34.2	0.0	11.2
M_{4v}	67.0	0.0	26.0	0.0	7.0
Γ_{3v}	5.4	0.7	91.8	2.1	0.0
Γ_{6v}	66.5	0.0	27.4	0.0	6.0
Γ_{1v}	73.8	0.0	23.5	2.0	0.7
Γ_{5v}	69.5	0.0	29.4	0.0	1.1

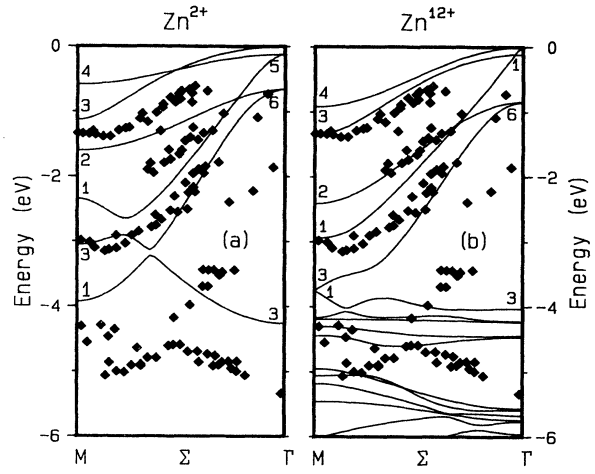

FIG. 3. Calculated electronic bands for ZnO along the Σ symmetry line in comparison with experimental data of Ref. 2. The bands have been computed using a Zn^{2+} potential in (a) and a Zn^{12+} potential in (b).

culations yielded metallic oxides in complete disagreement with experiment. Self-interaction-correction[21] (SIC) calculations for those oxides[34] and for a high-T_c cuprate[37] led to an opening of the gap and yielded results in much closer agreement with experiment. The analysis of the orbital character of some representative states, given in Table VI, clearly shows a very significant amount of p-d hybridization in the upper valence bands. The d admixture in many of these states amounts to almost 30%, which is twice as large as in ZnS and some states at the bottom of the p bands are resonant with the d level and show extremely large d admixtures. So any inaccuracies in the description of the highly localized Zn 3d bands by the LDA are transferred to a certain extent into the O 2p-derived valence bands by this strong p-d mixing. The strong d admixture and the Zn 4p contributions in the upper valence bands are of further importance in another context. An earlier empirical tight-binding calculation of surface states at ZnO ($10\bar{1}0$) retained only the O 2p orbitals[7] and another paper included hybridization between Zn 4p and O 2p orbitals in the upper valence-band states.[6] The two approaches lead to conflicting conclusions concerning the energetic position of anion-derived surface states near the gap energy region.[6,7] In fact, our results show that both empirical tight-binding Hamiltonians used in Refs. 6 and 7 cannot describe the underlying physics properly since they neglect the Zn 3d contributions to the bonding in ZnO.

Experimental ARPES data for ZnO are available along the Γ M symmetry line.[2] We compare these data in Fig. 3(a) with the electronic bands calculated with the Zn^{2+} potential. The agreement of the band dispersions with experiment is very poor and the calculated valence band width is too small by more than 1 eV. In Fig. 3(b) we compare the calculated bands for the Zn^{12+} potential with the same data set. Due to the p-d interaction the upper four valence bands now show much stronger dispersions. The agreement with experiment is considerably improved. The energetic separation of the two highest occupied bands could not be resolved in experiment.[2] The agreement between theory and experiment for the lower two p-derived valence bands in Fig. 3(b) is still very unsatisfactory, in particular in view of the fact that the measured bands are not to be interpreted in terms of Zn 3d bands. The latter were found between -9.5 and -6 eV in Ref. 2, as discussed already. These two measured bands certainly are the lowest two valence bands mostly derived from the O 2p and Zn 4s states. The p-d interaction increases the width of these bands only little with respect to the results for Zn^{2+}. This is partly a consequence of the d-band positions which are too high in energy in our results.

We have tested band-structure changes if the d bands are shifted to lower energies within LDA-type calculations. This can be achieved by carrying out LDA calculations using a Slater X_α potential[38] instead of the Ceperley-Alder exchange and correlation potential.[20,21] The value $\alpha=\frac{2}{3}$ obtains to the "exchange-only" potential derived for the homogeneous electron gas.[39] By increasing the potential parameter α we can simulate correlation effects, which are more important for extremely localized than for extended states. With $\alpha=0.7$ we obtain a band structure very similar to that using the Zn^{12+} ionic pseudopotential together with the Ceperley-Alder exchange-correlation functional. For $\alpha=0.9$ the d bands are shifted downwards by 0.7 eV and separate from the lower s-p-derived valence bands. This is accompanied by an increased valence bandwidth of 4.6 eV. The size of the optical gap increases to 1.58 eV. At the same time, the dispersions of the mainly oxygen-derived states at the top of the valence bands decrease and show less good agreement with the experimental data. Using even larger values for α, we find the d bands to shift further down in energy and the optical gap to further open up. The width of the upper six valence bands does become smaller again. A better description of the upper valence bands and of the d bands calls for an explicit inclusion of many-body correlation effects or, in particular, for an exchange-correlation functional that allows for a better description of highly localized and correlated states. One promising road for such calculations going beyond LDA

could be LDA-SIC calculations similar to the ones reported by Svane and Gunnarson in Refs. 34 and 37 whose results show a number of SIC-induced trends pointing altogether in the right direction.

In spite of the shortcomings mentioned, our calculations with a Zn^{12+} ionic pseudopotential yield the correct lattice constants and a reliable description of the occupied states near the fundamental gap. This is of basic importance for the determination of surface structures from total energy minimizations and for the identification of electronic surface states near the gap energy region. Furthermore, our results are obtained by state of the art LDA calculations and define an optimal starting point for investigations of correlation effects in ZnO by going beyond LDA using for example the LDA-SIC approach.

Finally, we show in Fig. 4 the total valence charge densities for ZnS and ZnO as they result with the Zn^{2+} and the Zn^{12+} ionic pseudopotentials in direct comparison. The plots clearly reveal the strong ionic character of bonding in these hexagonal compound semiconductors. When the Zn^{2+} potential is used, the valence charge density is almost spherically symmetric and strongly localized around the anions. If the Zn^{12+} pseudopotential is used, the charge density around the anions is changed only marginally. In this case, however, there occurs a spherically symmetric high charge density at each Zn cation which shows the closed shell of the Zn $3d$ electrons. Interestingly enough, the total valence charge densities in Fig. 4 indicate that the bonding in ZnS has more covalent character than in ZnO.

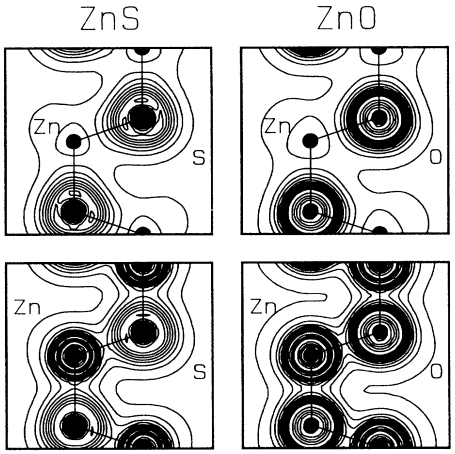

FIG. 4. Total valence charge densities for ZnS and ZnO. The upper two contour plots result from the Zn^{2+} and the lower two plots from the Zn^{12+} pseudopotential calculations. Due to the enormous differences between the charge densities of O, S, and Zn we have chosen three different spacings for the contours to illustrate the structure of the densities. The values of the maximum contours are 4.85, 0.85, and 0.17 for the Zn^{12+}, O^{6+} and S^{6+} ions. The units are e/a.u.^{3} Starting with the lowest contour (0.01) a spacing of 0.02 is used up to 0.25. The following contours are spaced by 0.15 and from the 0.85 contour by 0.8. It should be noted that the length scales are different for ZnS and ZnO according to the different lattice constants.

IV. SUMMARY

In conclusion, we have reported the first *ab initio* studies of the wurtzite-structure compounds ZnS and ZnO. We have shown that the explicit consideration of the Zn $3d$ electrons as valence electrons is a necessary step towards a quantitative description of the structure and the electronic properties of these compounds. There occurs a considerable p-d interaction giving rise to about 15% (30%) d admixture in the wave functions of the upper six anion-p-derived valence bands in ZnS (ZnO). The d electrons increase the lattice constants by 13% and 22%, respectively, as compared to calculations with the Zn^{2+} potential. Our calculated lattice constants agree extremely well with experiment when the Zn^{12+} ionic pseudopotential is used. For ZnS, the electronic band structure is found to be in good general agreement with data for cubic ZnS , except for the gap energy and the energetic position of the Zn $3d$ bands. These shortcomings both originate from the use of the LDA. For ZnO the uppermost four valence bands are found in reasonable agreement with experiment. In this case, not only the gap energy and the position of the Zn $3d$ bands are unsatisfactory, but also the energy position of the lower two mainly O $2p$-derived valence bands. It was argued that these discrepancies originate from correlation effects. The Zn $3d$ eigenstates are strongly correlated and highly localized. In ZnO they are nearly resonant with the O $2p$ energy levels, in addition. Therefore the observed discrepancies between our LDA results and the experimental data are considerably larger in ZnO than in ZnS.

ACKNOWLEDGMENT

Financial support by the Deutsche Forschungsgemeinschaft under Grant No. Po 215/5-1 is gratefully acknowledged.

APPENDIX: EVALUATION OF GAUSSIAN INTEGRALS INVOLVING SEPARABLE PSEUDOPOTENTIALS

The computational effort of an *ab initio* pseudopotential calculation is substantially reduced if separable instead of the standard nonlocal pseudopotentials[16,40–43] are used. This holds for computations using a plane-wave basis as well as for calculations carried out in a Gaussian basis which is used in this work. The evaluation of the Hamiltonian matrix elements involves integrals of the form

$$I_{\alpha\beta}^{AB}=\int\int \Phi_\alpha^*(\mathbf{r}-\mathbf{A})V_{KB}(\mathbf{r},\mathbf{r}')\Phi_\beta(\mathbf{r}'-\mathbf{B})d^3r d^3r' \ , \quad \text{(A1)}$$

with Gaussian orbitals of symmetry type α (β) located at $\mathbf{A}$ ($\mathbf{B}$). V_{KB} is the nonlocal pseudopotential in the separable form suggested by Kleinman and Bylander,[17]

$$V_{\mathrm{KB}}(\mathbf{r},\mathbf{r}')=V_{\mathrm{local}}(\mathbf{r})\delta(\mathbf{r}-\mathbf{r}') + \sum_l \sum_{m=-l}^{l} U_l(r)R_l(r)Y_{l,m}(\Theta,\varphi) \times Y_{l,m}^*(\Theta',\varphi')U_l(r')R_l^*(r') \ . \quad \text{(A2)}$$

Y_{lm} are the spherical harmonics and $R_l(r)$ are the solu-

tions of the radial Schrödinger equation

$$\left[-\frac{\hbar^2}{2M}\frac{d^2}{dr^2}+\frac{\hbar^2}{2M}\frac{l(l+1)}{r^2}+V_l^{\mathrm{PS}}(r)\right]rR_l(r)=E_l rR_l(r) \tag{A3}$$

for a standard pseudopotential. The U_l are defined by

$$U_l(r)=\frac{V_l^{\mathrm{PS}}(r)-V_{\mathrm{local}}(r)}{\left[\int R_l^*(r)[V_l^{\mathrm{PS}}(r)-V_{\mathrm{local}}(r)]R_l(r)r^2dr\right]^{1/2}} . \tag{A4}$$

Inserting V_{KB} into the atomic problem (A3) it is easily seen that the radial Schrödinger equation for each l is satisfied by this construction. The choice of the local part V_{local} is arbitrary.[17] In many approaches[17,18,43,44] V_{local} was successfully set to the highest angular component of the standard pseudopotential. However, in the case of Zn^{12+} we have chosen the $l=0$ component as the local potential in order to avoid ghost states[19] and in order to create a very smooth local part of V_{KB}. Due to the separable form of V_{KB} Eq. (A1) takes the form

$$I_{\alpha\beta}^{AB}=\int\Phi_\alpha^*(\mathbf{r}-\mathbf{A})V_{\mathrm{local}}(r)\Phi_\beta(\mathbf{r}-\mathbf{B})d^3r + \sum_l\sum_{m=-l}^{l}F(\alpha,\mathbf{A},l,m)F^*(\beta,\mathbf{B},l,m) , \tag{A5}$$

with

$$F(\alpha,\mathbf{A},l,m)=\int\Phi_\alpha^*(\mathbf{r}-\mathbf{A})U_l(r)R_l(r)Y_{l,m}(\Theta,\varphi)d^3r . \tag{A6}$$

The local part of (A5) is evaluated by transforming V_{local} into Fourier representation. The remaining integrals involving two Gaussians and a plane wave are solved analytically. U_l and R_l are given numerically on a dense grid either from the table of Stumpf, Gonze, and Scheffler[18] or from the explicit solution of (A3). The radial wave functions have the asymptotic form

$$\lim_{r\to0}R_l(r)\to r^l . \tag{A7}$$

We have fitted

$$U_l(r)R_l(r)=r^l\sum_{i=I}^{N}c_{i,l}\exp(-\gamma_{i,l}r^2)d^3r , \tag{A8}$$

using a nonlinear least-squares fit with $N=10$. The integrals (A6) take the form

$$F(\alpha,\mathbf{A},l,m)=\sum_{i=1}^{N}c_{i,l}\int\Phi_\alpha^*(\mathbf{r}-\mathbf{A})r^lY_{l,m}(\Theta,\varphi)\times\exp(-\gamma_{i,l}r^2)d^3r . \tag{A9}$$

The products $r^lY_{l,m}(\Theta,\varphi)$ are transformed into Cartesian coordinates and the integrals in (A9) have the same form as the overlap integrals which are easily evaluated analytically.

[1] J. E. Jaffe, R. Pandey, and A. B. Kunz, Phys. Rev. B **43**, 14 030 (1991).
[2] G. Zwicker and K. Jacobi, Solid State Commun. **54**, 701 (1985).
[3] W. Göpel, R. S. Bauer, and G. V. Hansson, Surf. Sci. **99**, 138 (1980).
[4] W. H. Cheng and H. H. Kung, Surf. Sci. **122**, 21 (1982).
[5] G. S. Rohrer and D. A. Bonnel, Surf. Sci. Lett. **247**, L195 (1991).
[6] Y. R. Wang and C. B. Duke, Surf. Sci. **192**, 309 (1987).
[7] I. Ivanov and J. Pollmann, Phys. Rev. B **24**, 7275 (1981).
[8] R. Kuwabara, H. Adachi, and T. Morimoto, Surf. Sci. **193**, 271 (1988).
[9] U. Rössler, Phys. Rev. **184**, 733 (1969).
[10] S. Bloom and I. Ortenburger, Phys. Status Solidi B **58**, 561 (1973).
[11] J. R. Chelikowsky, Solid State Commun. **22**, 351 (1977).
[12] J. D. Joannopoulos and M. L. Cohen, J. Phys. C **6**, 1572 (1973).
[13] *Numerical Data and Functional Relationships in Science and Technology,* Landolt-Börnstein, New Series Group III, Vol. 17a and 22a, edited by K.-H. Hellwege and O. Madelung (Springer, New York, 1982).
[14] R. Weidemann *et al.*, Phys. Rev. B **45**, 1172 (1992).
[15] P. Hohenberg and W. Kohn, Phys. Rev. **136**, B864 (1964); W. Kohn and L. J. Sham, *ibid.* **140**, A1133 (1965).
[16] D. R. Hamann, M. Schlüter, and C. Chiang, Phys. Rev. Lett. **43**, 1494 (1979).
[17] L. Kleinman and D. M. Bylander, Phys. Lett. **48**, 1425 (1982).
[18] R. Stumpf, X. Gonze, and M. Scheffler, Fritz Haber Institute Research Report, Berlin, 1990.
[19] X. Gonze, P. Käckell, and M. Scheffler, Phys. Rev. B **41**, 12 264 (1990).
[20] D. M. Ceperley and B. J. Alder, Phys. Rev. Lett. **45**, 566 (1980).
[21] J. P. Perdew and A. Zunger, Phys. Rev. B **23**, 5048 (1981).
[22] G. B. Bachelet, H. S. Greenside, G. A. Baraff, and M. Schlüter, Phys. Rev. B **24**, 4745 (1981).
[23] J. Ihm, A. Zunger, and M. L. Cohen, J. Phys. C **12**, 4409 (1979).
[24] D. J. Chadi and M. L. Cohen, Phys. Rev. B **8**, 5747 (1973).
[25] J. W. Cooley and J. W. Tukey, Math. Comput. **119**, 297 (1965).
[26] See, e.g., *Electronic Structure, Dynamics, and Quantum Structural Properties of Condensed Matter,* Vol. 121 of *NATO Advanced Study Institute, Series B: Physics,* edited by J. T. Devreese and P. van Camp (Plenum, New York, 1985).
[27] K. J. Chang, S. Froyen, and M. L. Cohen, Phys. Rev. B **28**, 4736 (1983).
[28] S. H. Wei and A. Zunger, Phys. Rev. B **37**, 8958 (1988).
[29] V. Fiorentini, M. Methfessel, and M. Scheffler (unpublished) have pointed out that a proper treatment of the *d* electrons is also essential for a resonable description of the structural properties of the III-V compound GaN.
[30] A. Zunger and A. J. Freemann, Phys. Rev. B **16**, 2901 (1977).
[31] M. S. Hybertsen and S. G. Louie, Phys. Rev. Lett. **55**, 1418 (1985); R. W. Godby, M. Schlüter, and L. J. Sham, *ibid.* **56**, 2415 (1986).
[32] J. L. Martins, N. Troullier, and S. H. Wei, Phys. Rev. B **43**, 2213 (1991).
[33] L. J. Raubenheimer and G. Gilat, Phys. Rev. **157**, 586 (1967).
[34] A. Svane and O. Gunnarsson, Phys. Rev. Lett. **65**, 1148 (1990).
[35] S. G. Louie, S. Froyen, and M. L. Cohen, Phys. Rev. B **26**,

2738 (1982).
[36]G. E. Engel and R. J. Needs, Phys. Rev. B **41**, 7876 (1990).
[37]A. Svane, Phys. Rev. Lett. **68**, 1900 (1992).
[38]J. C. Slater, Phys. Rev. **81**, 385 (1951).
[39]R. Gaspar, Acta Phys. Hung. **3**, 263 (1954).
[40]A. Zunger and M. L. Cohen, Phys. Rev. B **18**, 5449 (1978).
[41]G. P. Kerker, J. Phys. C **13**, L189 (1980).
[42]G. B. Bachelet, D. R. Hamann, and M. Schlüter, Phys. Rev. B **26**, 4199 (1982).
[43]D. R. Hamann, Phys. Rev. B **40**, 2980 (1989).
[44]N. Troullier and J. L. Martins, Phys. Rev. B **43**, 1993 (1991); **43**, 8861 (1991).